

Electrical Conductivity Changes During Irreversible Electroporation Treatment of Brain Cancer

Paulo A. Garcia, *IEEE Member*, John H. Rossmeisl, Jr., and Rafael V. Davalos, *IEEE Member*

Invited Paper

Abstract— Irreversible electroporation (IRE) is a new minimally invasive technique to kill tumors and other undesirable tissue in a non-thermal manner. During an IRE treatment, a series of short and intense electric pulses are delivered to the region of interest to destabilize the cell membranes in the tissue and achieve spontaneous cell death. The alteration of the cellular membrane results in a dramatic increase in electrical conductivity during IRE as in other electroporation-based-therapies. In this study, we performed the planning and execution of an IRE brain cancer treatment using MRI reconstructions of the tumor and a multichannel array that served as a stereotactic fiducial and electrode guide. Using the tumor reconstructions within our numerical simulations, we developed equations relating the increase in tumor conductivity to calculated currents and volumes of tumor treated with IRE. We also correlated the experimental current measured during the procedure to an increase in tumor conductivity ranging between 3.42-3.67 times the baseline conductivity, confirming the physical phenomenon that has been detected in other tissues undergoing similar electroporation-based treatments.

I. INTRODUCTION

IRREVERSIBLE electroporation (IRE) is a new technique that has shown great promise in the focal ablation of undesirable tissue [1]. The procedure involves placing minimally invasive electrodes within the region of interest and delivering a series of low-energy electric pulses [2, 3]. The pulses create an electric field that induces an increase in the resting transmembrane potential (TMP) of the cells in the tissue [3, 4]. The induced increase in the TMP is dependent on the electric pulse parameters. Depending on the magnitude of the induced TMP the electric pulses can have no effect, transiently increase membrane permeability or cause spontaneous cell death [5]. When the magnitude of the induced transmembrane potential is above a critical value, the cell membrane is disrupted to such an extent that the cell dies due to loss of homeostasis [5]. Consequently, the treated regions are sharply delineated and can be predicted with numerical models that simulate the electric field distributions in tissue [6]. One of the main advantages of IRE over other focal ablation techniques is that the therapy

does not use thermal damage from resistive heating to kill the cells. Thus major blood vessels, extracellular matrix and other tissue structures are spared [7].

Our group has confirmed that the procedure can be used safely in the brain and is well-tolerated in normal canine subjects [7]. Prior to our studies, the use of IRE ablation of tissue in the CNS has never been reported. We conducted a pilot study on four canines to determine the effects of IRE in the brain [7]. Confirming results attained by other investigations in other tissues [1, 2], our results show that IRE is readily capable of killing brain tissue and spares major brain vasculature making IRE appropriate for treatment of tumors adjacent to, or enveloping critical vascular structures. Our results also showed sharp sub-millimeter delineation between treated and non-treated tissue. The technique also provides the ability for the neurosurgeon to visualize the treatment region with medical images including magnetic resonance imaging (MRI), ultrasound (US) and computed tomography (CT) and retreat if necessary in order to ensure coverage of the entire region of interest.

We successfully treated a canine patient with IRE and radiation therapy for a non-resectable, forebrain high-grade/malignant glioma, resulting in complete remission of the tumor at four months [8]. We performed the IRE procedure at the time of biopsy with treatment parameters derived from treatment planning numerical models and preliminary data in normal brain [7, 9]. The IRE ablation procedure resulted in nearly complete resolution of focal neurological dysfunction, attributed to the tumor, within one week of the procedure. An MRI scan of the brain, performed 3 days post-surgery, demonstrated a 75% reduction in 3D tumor volume. The canine patient subsequently received adjunctive fractionated whole-brain radiotherapy for 4 weeks following IRE therapy (50 Gy, delivered in 20 fractions of 2.5 Gy each), resulting in complete remission 4 months after the IRE therapy, based on serial MRI and neurologic examinations. It is unclear whether the complete response at 4 months was a result of IRE alone or the combination therapy due to the limited assessments between the two time points. Therefore, it is imperative to determine the efficacy of IRE for brain cancer treatment in isolation and combination with current standards of care. In this study we demonstrate how one can perform the planning for brain cancer IRE treatment by simultaneously using MRI tumor reconstructions from three perpendicular planes. Additionally, we used an implanted catheter array as a stereotactic fiducial that enabled us to perform a minimally invasive procedure with CT-guidance for electrode

Manuscript received March 26, 2011. This work was supported in part by the Coulter Foundation and by the NSF CBET-0933335.

R.V. Davalos, Ph.D., and P.A. Garcia, Ph.D., are with the Virginia Tech-Wake Forest University School of Biomedical Engineering and Sciences, Blacksburg, VA 24061 USA (phone:540-231-1979, email: davalos@vt.edu; pgarcia@vt.edu).

J.H. Rossmeisl, Jr., D.V.M., M.S. is with the Virginia-Maryland Regional College of Veterinary Medicine, Blacksburg VA 24061 USA (jrossmei@vt.edu).

placement and outcome assessment. Finally, we present results correlating the change in tumor electrical conductivity due to electroporation, the measured current, and the volume of tumor treated with IRE. The results presented here support our hypothesis that IRE is a viable and independent option to treat brain cancer.

II. MATERIALS AND METHODS

A. Treatment Planning/Numerical Modeling

Open source image analysis software (OsiriX, Geneva, Switzerland) was used to reconstruct and calculate the tumor volumes. The tumor was reconstructed from the axial, sagittal, and coronal planes using the 0.2 T T2-weighted MRI scans. The veterinary neurosurgeon outlined the region of interest in each of the 2D pre-operative MRI scans and a 3D solid representation of the tumor was generated as in [7].

The 3D tumor reconstructions were imported into Comsol Multiphysics v.3.5a (Stockholm, Sweden). Each of the three reconstructions were scaled, rotated, and translated so that the tumor from the MRI and Comsol had the same volume, orientation and center of mass. The tumor target was fitted with a 1.2 cm x 2.0 cm x 2.6 cm ellipsoid for computational efficiency within a 5.0 cm x 5.0 cm x 7.0 cm brain domain and shown in Fig. 1A.

The electric field distribution associated with the electric pulse is given by solving the governing Laplace equation:

$$\nabla \cdot (\sigma \nabla \phi) = 0 \quad (1)$$

where σ is the electrical conductivity of the tissue and ϕ is the electrical potential [5]. The baseline electrical conductivity of the non-permeabilized brain and tumor tissues were 0.258 S/m and 0.43 S/m, respectively. These values were based on measurements by Latikka *et al.* in living humans at 37 °C [10, 11]. We chose the highest value from the literature for the electric conductivity of the tumor since there was significant edema. The electrical conductivity of the electrodes and insulation were set to 2.22×10^6 S/m and 1×10^{-5} S/m, respectively [9]. The electrical boundary condition along the tissue in contact with the energized electrode is $\phi = V_0$ and $\phi = 0$ at the other electrode. The boundaries where the analyzed domain is not in contact with an electrode are treated as electrically insulative.

The electrical conductivity of the tissue is dependent on the degree of electroporation [4]. Therefore, the electrical conductivity took into account these effects and is given by:

$$\sigma(E) = \sigma_0 [1 + F \cdot \text{flc2hs}(E - E_{\text{delta}}, E_{\text{range}})] \quad (2)$$

where σ_0 is the baseline conductivity and F the conductivity factor. The smoothed Heaviside function, flc2hs , changes from zero to one when $E - E_{\text{delta}} = 0$ over the range $\pm E_{\text{range}}$. In the simulations we used a value $E_{\text{delta}} = 580$ V/cm and $E_{\text{range}} = 120$ V/cm in order to match those used by Sel *et al.* [4, 9]. The volume of tumor treated with IRE and the total current were calculated for conductivity factors ranging between 0-3.

B. Clinical Procedure

A 7-year old neutered male canine patient (Labrador Retriever) was referred to the Virginia-Maryland Regional College of Veterinary Medicine for IRE therapy following

poor clinical response and progressive growth of a high grade astrocytoma. This canine had failed to respond to surgical resection and two separate protocols of experimental immunotherapy and intratumoral chemotherapy, administered at other institutions over a 9-month interval.

This study was approved by the Institutional Animal Care and Use Committee with written, informed client consent. After induction of general anesthesia, a routine rostral approach to the right side of the skull was made on the dorsal midline through a previous skin incision. Two 1.5 mm channels were drilled within a previously implanted multichannel catheter array, which served as a stereotactic fiducial.

Two 1-mm in diameter blunt-tipped electrodes were guided 1.95 cm from the deep distal end of the catheter array to a location within the center of the tumor mass based on pre-operative treatment plans and stereotactic coordinates. The electrode locations were confirmed with intra-operative CT guidance. The electrodes had 5 mm exposed tips and had a center-to-center distance of 5 mm.

After confirmation of neuromuscular blockade to suppress patient motion prior to the IRE treatment, four sets of 20 pulses were delivered with the NanoKnife® generator (AngioDynamics, Queensbury, NY USA) with an applied voltage of 625 V. The electrodes were then advanced an additional 1.2 cm along the same trajectory to independently treat the more rostral and deeper aspects of the tumor. After confirmation of the desired electrode location with intra-operative CT, four sets of 20 pulses were delivered with an applied voltage of 500 V to this second treatment location. The polarity of the electrodes was alternated between the sets to minimize charge build-up on the electrode surface. The 50 μ s pulses were synchronized with the canine's heart rate in order to prevent cardiac arrhythmias and were delivered in sets of ten at approximately 1 Hz. Due to recharging demands of the capacitors, each set was delivered 3.5 seconds after the completion of the previous set. The IRE therapy was completed without visible patient motion or complications. The electrodes and temperature probes were withdrawn from the brain parenchyma, the catheter array capped, and a CT of the brain with IV contrast performed.

III. RESULTS

A. Treatment Planning/Numerical Modeling

Fig. 1 shows the tumor, brain, multichannel catheter array and electrodes used during the treatment planning. The 3D reconstructed tumor volumes were 2.85, 3.67, and 4.50 cm³ for the axial, sagittal, and coronal planes, respectively. The coordinates of the center of mass of the tumor was calculated from 4 axial, 5 sagittal, and 8 coronal slices. The center of mass of the multichannel catheter array was determined from a sagittal slice in which the cross-section of the device was largest. The simulated electric field distribution can be seen in Fig. 1B in which only the upper right portion of the tumor was targeted with the 625 V treatment, while avoiding any deleterious effects on the surrounding normal brain.

The increase in tumor electrical conductivity was evaluated numerically. Fig. 2 shows the calculated current and volumes of tumor treated with IRE as a function of the conductivity factor. We report the IRE treated volumes as those exposed to a minimum electric field of 500 V/cm since the IRE threshold for brain tumor tissue is currently not known [9]. The volume treated with IRE was 0.15-0.24 cm³ for 500 V and 0.24-0.4 cm³ for 625 V. The currents were 0.83-2.35 A and 1.13-3.49 A for the applied 500 and 625 V, respectively.

B. Clinical Procedure

The patient was recovered from anesthesia and within four hours, the canine was conscious. The pre-treatment tumor biopsy was diagnosed as high grade astrocytoma. Fig. 3A shows the CT scan used for confirmation of the electrode placement before the 625 V treatment. Fig. 3B displays the region of enhancement in CT post-contrast 30 minutes after the 500 V treatment. The volumes of tumor treated were calculated using the post-IRE contrast enhanced CT and resulted in 0.221 ± 0.006 and 0.254 ± 0.007 cm³ for the 500 and 625 V applied voltages, respectively.

The voltage and current measurements by the NanoKnife[®] during the IRE procedures are given in Table I. The conductivity factor was calculated for each treatment using the measured current and the equations from Fig. 2. Our results suggest that the brain tumor conductivity increases by 3.42-3.67 times the baseline conductivity as a result of electroporation. These values are in agreement with those reported for other organs in which the tissue or tumor increases by 3.0-3.6 times after electroporation [12]. The measured temperature ranged between 31.1°C and 36.5°C during the pulse delivery.

Table I: Calculated conductivity factor using *in vivo* current

Depth	Voltage (V)	Current (A)	Factor (F)
1 – 1.95 cm	627	3.24 ± 0.2	2.67 x
2 – 3.15 cm	514	2.08 ± 0.2	2.42 x

IV. DISCUSSION

This study provides several important considerations when performing IRE treatment planning in the brain. First, the tumor reconstruction from medical images such as MRI and CT should use several imaging planes in order to generate a reliable coordinate system and a comprehensive tumor target. This is important for electrode positioning, ensuring complete coverage of the target, and minimizing damage to surrounding normal tissue. The fiducial for guiding the electrodes into the tumor was crucial because it provided a stereotactic reference during treatment. Future work will include a more robust reconstruction platform for greater accuracy in electroporation-based treatment planning.

The change in tumor conductivity due to electroporation may have significant effects in treatment. We confirmed that brain tumor responds to electroporation-based therapies in a similar manner and these changes may have significant impact in the treatment outcome. The threshold for brain tumor tissue is currently unknown, and this is a limitation of

the current study. The experimental current, calculated volumes of CT enhancement, and the curves in Fig. 2A provide insight as to the relative magnitude needed for brain tumor ablation with IRE volumes specifically in the 500 V case. The discrepancy between the experimental and numerical IRE volumes for the 625 V (Fig. 2B) suggest that the threshold for tumor tissue was higher than the assumed 500 V/cm. Determining the conductivity for brain tissue as a function of electric field and the threshold for tumors are needed for clinical applications of intracranial IRE. Once these thresholds are established and a more robust treatment planning platform implemented, it may be possible to accurately predict treatment outcome by measuring the current during intracranial procedures and re-treat if the expected changes are not detected.

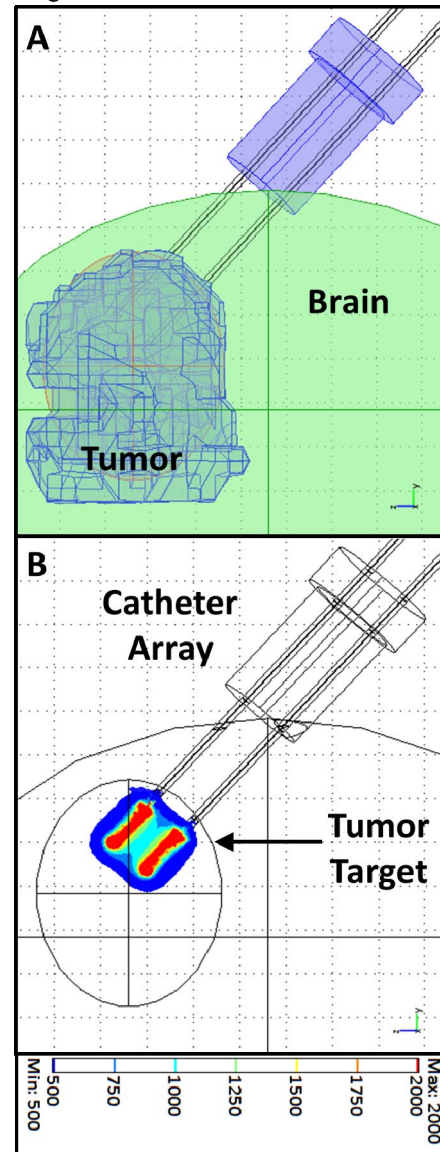


Fig. 1: IRE treatment planning for a brain cancer patient with A) MRI reconstructed tumor and corresponding B) electric field [V/cm] distribution within the tumor target.

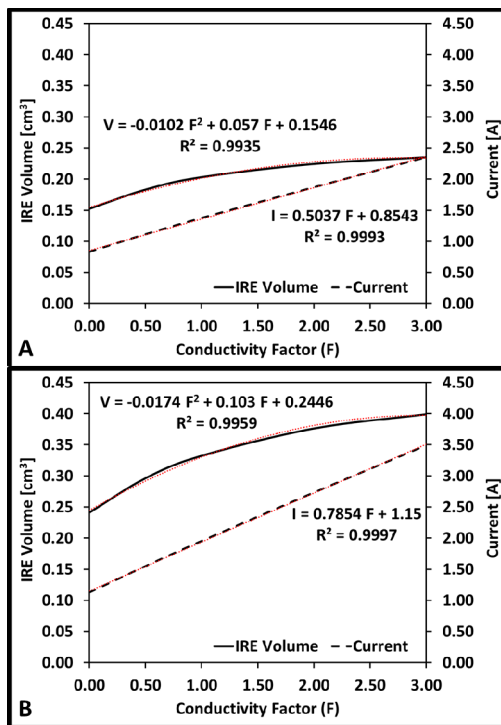


Fig. 2: Numerical results relating the increase in tumor conductivity with treated volume and current for the A) 500 V and B) 625 V IRE treatments.

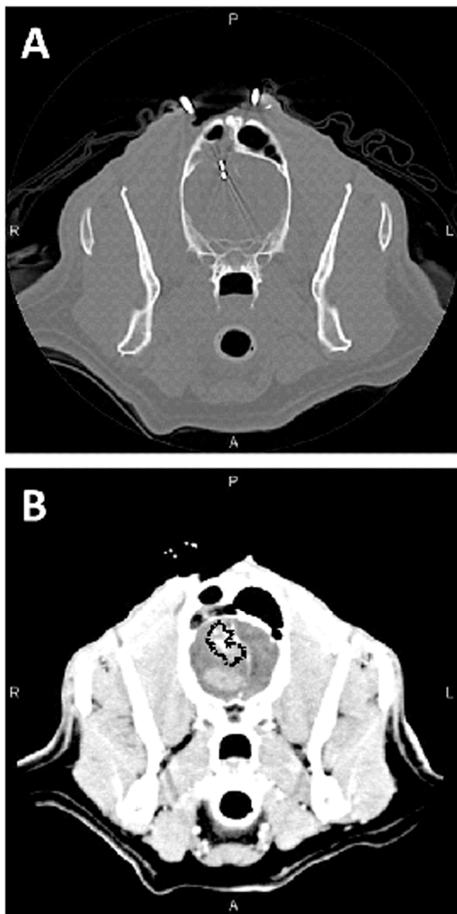


Fig. 3: IRE procedure performed with CT-guidance A) electrode placement and B) treatment visualization.

ACKNOWLEDGMENT

The authors thank T. Pancotto and N. Henao-Guerrero for their assistance in surgery and J. Robertson, R.E Neal II, and A. Rojas for their help during the procedure.

REFERENCES

- [1] J.F. Edd, L. Horowitz, R.V. Davalos, L.M. Mir, and B. Rubinsky, "In vivo results of a new focal tissue ablation technique: irreversible electroporation," *IEEE Trans Biomed Eng*, 53, 1409-15, Jul 2006.
- [2] B. Al-Sakere, F. Andre, C. Bernat, E. Connault, P. Opolon, R.V. Davalos, B. Rubinsky, and L.M. Mir, "Tumor ablation with irreversible electroporation," *PLoS ONE*, 2, e1135, 2007.
- [3] J.C. Weaver, "Electroporation of biological membranes from multicellular to nano scales," *IEEE T Dielect El In*, 10, 754-768, 2003.
- [4] D. Sel, D. Cukjati, D. Batuskaite, T. Slivnik, L.M. Mir, and D. Miklavcic, "Sequential finite element model of tissue electropermeabilization," *IEEE Trans Biomed Eng*, 52, 816-27, May 2005.
- [5] R.V. Davalos, L.M. Mir, and B. Rubinsky, "Tissue ablation with irreversible electroporation," *Ann Biomed Eng*, 33, 223-31, Feb 2005.
- [6] D. Miklavcic, K. Beravs, D. Semrov, M. Cemazar, F. Demsar, and G. Sersa, "The importance of electric field distribution for effective in vivo electroporation of tissues," *Biophysical Journal*, 74, 2152-2158, 1998.
- [7] T.L. Ellis, P.A. Garcia, J.H. Rossmeisl, N. Henao-Guerrero, J. Robertson, and R.V. Davalos, "Nonthermal irreversible electroporation for intracranial surgical applications," *J Neurosurg*, 114, 681-688, 2011.
- [8] P.A. Garcia, T. Pancotto, J.H. Rossmeisl, N. Henao-Guerrero, N.R. Gustafson, G.B. Daniel, J.L. Robertson, T.L. Ellis, and R.V. Davalos, "Non-thermal irreversible electroporation (N-TIRE) and adjuvant fractionated radiotherapeutic multimodal therapy for intracranial malignant glioma in a canine patient," *Technol Cancer Res Treat*, 10, 73-83, 2011.
- [9] P.A. Garcia, J.H. Rossmeisl, R.E. Neal II, T.L. Ellis, J. Olson, N. Henao-Guerrero, J. Robertson, and R.V. Davalos, "Intracranial nonthermal irreversible electroporation: In vivo analysis," *J Membr Biol*, 236, 127-136, 2010.
- [10] C. Gabriel, A. Peyman, and E.H. Grant, "Electrical conductivity of tissue at frequencies below 1 MHz," *Phys Med Biol*, 54, 4863-78, Aug 21 2009.
- [11] J. Latikka, T. Kuurne, and H. Eskola, "Conductivity of living intracranial tissues," *Phys Med Biol*, 46, 1611-6, Jun 2001.
- [12] D. Miklavcic, M. Snoj, A. Zupanic, B. Kos, M. Cemazar, M. Kropivnik, M. Bracko, T. Pecnik, E. Gadzijev, and G. Sersa, "Towards treatment planning and treatment of deep-seated solid tumors by electrochemotherapy," *BioMedical Engineering OnLine*, 9, 10, 2010.